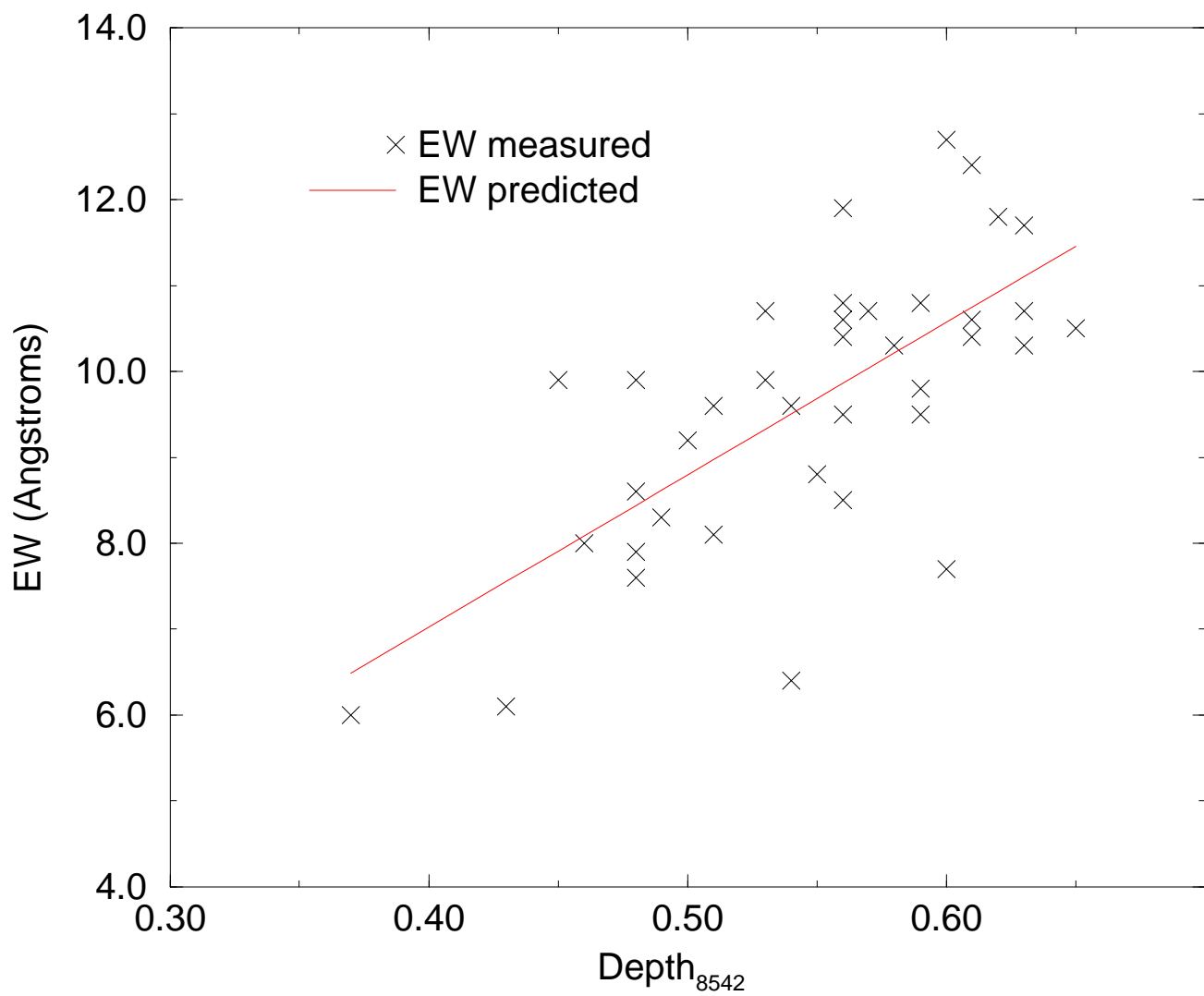


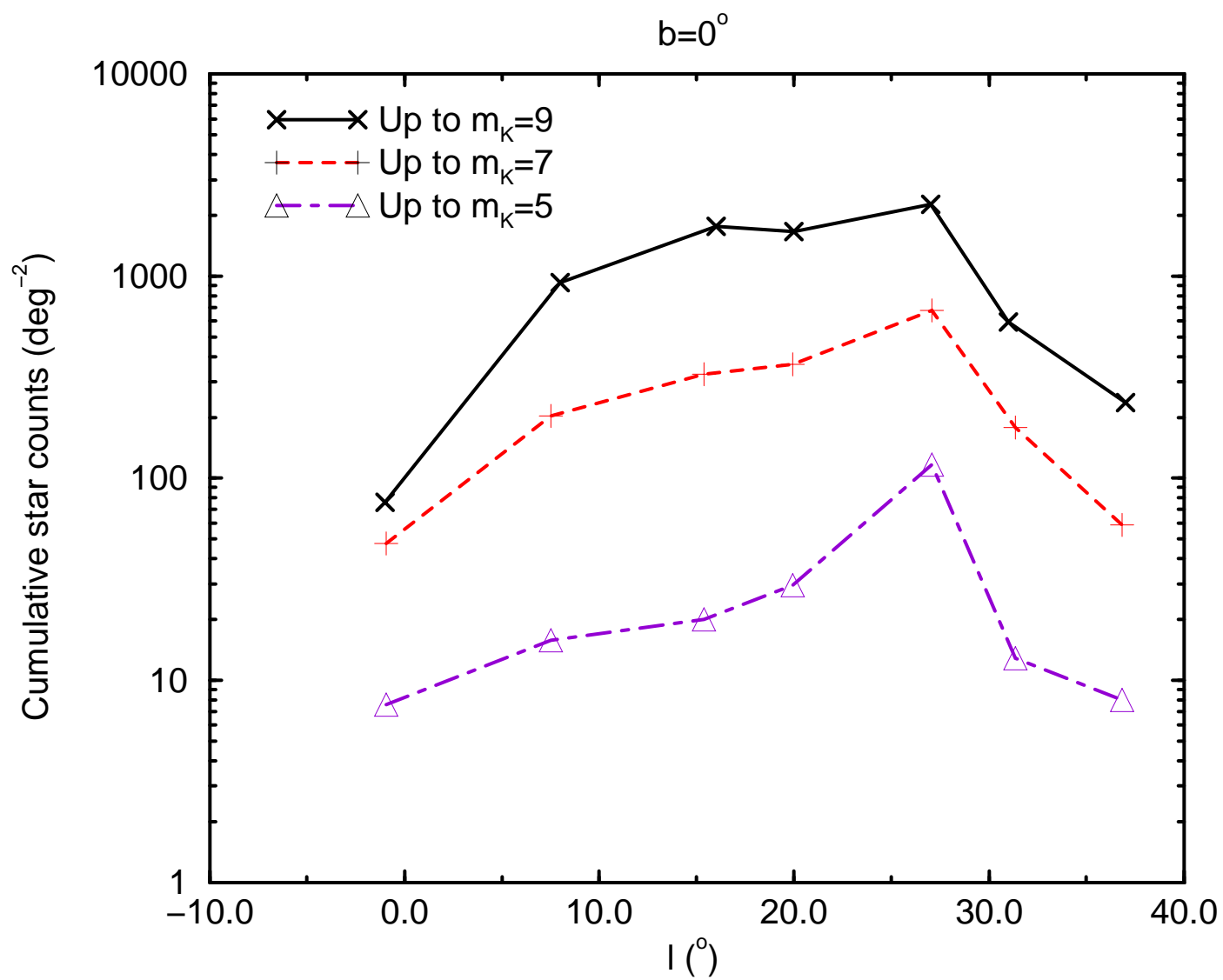
Table 1: List of stellar characteristics of the stars sample: coordinates J2000, equivalent width  $EW$ , equation used to derive  $EW$ , luminosity class, spectral type and distance (G97).  
NOTE: Investigators who may wish to use the coordinates should be aware that due to the intrinsic unaccuracies of the TMGS coordinates and the extreme crowding in the field there is often more than one visible candidate for the IR source.

#	RA( <sup>h</sup> <sup>m</sup> <sup>s</sup> ),dec( <sup>°</sup> ' ")	$m_K$	$EW$	$EW$ from eq..	Lumin. class	Spectral type	dist. (kpc)
1	18 30 28.2, -5 12 34	3.90	9.2	(2)	I	K5	3.8
2	18 30 52.9, -5 08 24	4.40	8.6	(5)	III	M7	6.9
3	18 31 57.2, -5 13 05	2.50	11.8	(2)	I	K5	2.3
4	18 32 04.3, -5 13 31	4.30	9.3	(5)	I	M3	7.9
5	18 32 17.6, -5 12 34	4.50	11.7	(2)	I	K5	4.7
6	18 32 21.3, -5 14 51	4.10	9.9	(2)	I	K2	4.1
7	18 32 29.0, -5 16 50	4.20	9.8	(2)	I	K5	4.3
8	18 32 33.2, -5 16 49	4.10	8.6	(5)	III	M8	6.3
9	18 32 34.4, -5 14 49	3.80	9.9	(2)	I	F5	1.4
10	18 33 05.3, -5 17 40	4.80	9.6	(2)	I	K5	5.1
11	18 33 06.9, -5 09 47	4.28	8.1	(2)	III	K2	1.2
12	18 34 35.2, -5 11 56	4.74	9.5	(5)	I	M6	8.5
13	18 34 37.3, -5 15 05	3.60	7.7	(5)	III	M5	2.9
14	18 35 12.5, -5 17 44	3.90	8.0	(2)	III	K0	0.8
15	18 35 35.3, -5 04 01	4.25	9.3	(5)	I	M6	7.9
16	18 35 36.0, -5 03 57	3.70	9.2	(5)	I	M4	6.9
17	18 35 45.4, -5 20 15	4.00	12.7	(2)	I	K5	4.1
18	18 36 23.0, -5 07 04	4.58	10.5	(2)	I	G5	1.9
19	18 37 17.7, -5 16 12	2.20	10.3	(2)	I	K2	2.0
20	18 37 26.0, -5 05 08	4.90	9.3	(5)	I	M8	9.9
21	18 37 45.9, -5 20 29	4.80	9.6	(2)	I	G8	2.1
22	18 37 53.2, -5 04 32	5.00	8.6	(5)	III	M6	7.5
23	18 37 54.5, -5 14 48	3.30	10.8	(2)	I	K2	3.1
24	18 38 05.7, -5 19 37	4.80	10.4	(2)	I	K0	5.2
25	18 38 23.8, -5 15 42	4.52	9.5	(5)	I	M8	8.1
26	18 38 39.2, -5 12 22	4.72	10.6	(2)	I	M0	5.2
27	18 38 50.4, -5 12 31	2.30	11.9	(2)	I	K2	2.1
28	18 39 05.4, -5 12 28	3.70	10.6	(2)	I	K2	3.6
29	18 39 07.1, -5 15 43	4.34	< 10.2	(5)	I/III	M8	–
30	18 39 28.2, -5 14 47	4.90	12.4	(2)	I	K5	5.4

Continuation of Table 1.

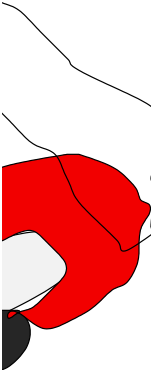
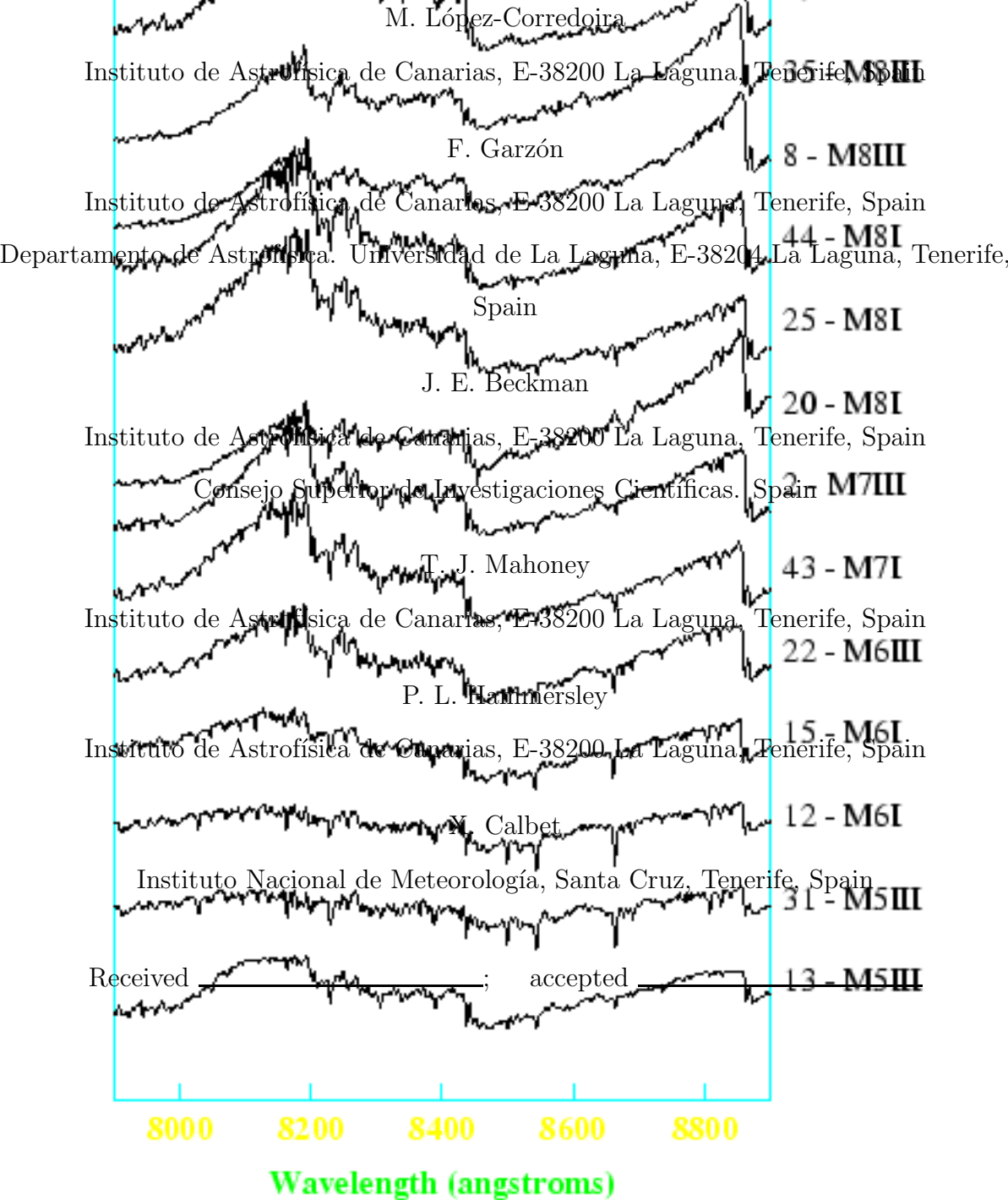
#	RA( <sup>h</sup> <sup>m</sup> <sup>s</sup> ),dec( <sup>°</sup> ' ")	$m_K$	$EW$	$EW$ from eq..	Lumin. class	Spectral type	dist. (kpc)
31	18 39 32.9, -5 15 19	4.80	8.9	(5)	III	M5	7.5
32	18 39 36.1, -5 16 48	5.00	10.7	(2)	I	K2	5.7
33	18 39 49.8, -5 18 20	2.10	6.0	(2)	III	M2	0.2
34	18 39 58.2, -5 16 45	4.80	9.9	(2)	I	K2	5.2
35	18 40 01.0, -5 14 11	3.60	8.6	(5)	III	M8	5.2
36	18 40 01.7, -5 13 01	5.00	8.6	(2)	III	K0	2.8
37	18 40 38.2, -5 06 45	4.74	< 10.2	(5)	I/III	M9	–
38	18 40 49.0, -5 05 23	4.76	6.4	(2)	III	M3	0.9
39	18 40 49.1, -5 05 28	4.60	7.6	(2)	III	G5	0.3
40	18 41 21.2, -5 16 17	4.26	9.5	(2)	I	G2	1.7
41	18 41 55.7, -5 14 16	4.50	10.8	(2)	I	G5	1.8
42	18 42 03.6, -5 04 54	4.36	6.4	(5)	III	M3	0.8
43	18 42 14.3, -5 11 30	4.35	9.9	(5)	I	M7	7.5
44	18 42 17.8, -5 13 06	4.42	9.2	(5)	I	M8	7.5
45	18 42 35.1, -5 16 50	4.42	8.8	(2)	III	K2	2.9
46	18 42 50.2, -5 18 23	4.65	10.7	(2)	I	G2	1.9
47	18 43 15.5, -5 17 48	4.51	9.4	(5)	I	M5	7.7
48	18 43 25.9, -5 11 33	4.40	8.9	(5)	III	M4	6.9
49	18 44 26.2, -5 14 49	4.31	10.3	(2)	I	G5	1.7
50	18 44 47.1, -5 14 51	4.35	9.5	(2)	I	K3	4.6
51	18 45 08.7, -5 12 34	4.45	10.7	(2)	I	G2	1.8
52	18 45 12.4, -5 16 50	4.30	7.9	(2)	III	G5	0.4
53	18 45 34.2, -5 12 33	4.62	6.1	(2)	III	G5	0.1
54	18 45 40.0, -5 07 00	4.46	10.4	(2)	I	G1	1.8
55	18 45 41.9, -5 14 48	4.31	8.5	(2)	III	K3	2.0
56	18 45 43.9, -5 15 21	4.20	9.9	(5)	I	M4	6.9
57	18 45 47.1, -5 17 45	4.69	9.3	(5)	I	M4	9.7
58	18 45 53.6, -5 21 05	4.52	8.3	(2)	III	K7	2.1
59	18 51 37.1, -5 20 11	4.33	7.7	(2)	III	F7	0.3
60	18 54 39.8, -5 11 43	4.39	9.3	(5)	I	M9	8.3





A major star formation region in the receding tip of the stellar  
Galactic bar.

II. Supplementary information and evidence that the bar is not  
the same structure as the triaxial bulge previously reported.



Dust  
bulge

utum

## ABSTRACT

This paper is the second part of Garzón *et al.* (1997) in which we presented an outline of the analysis of 60 spectra from a follow-up program to the Two Micron Galactic Survey (TMGS, Garzón *et al.* 1993) project in the  $\ell = 27^\circ$ ,  $b = 0^\circ$  area. In this second part, we present a more detailed explanation of the analysis as well a library of the spectra for more complete information for each of the 60 stars, and further discussions on the implications for the structure of the Galaxy.

This region contains a prominent excess in the flux distribution and star counts previously observed in several spectral ranges, notably in the TMGS. More than 50% of the spectra of the stars detected with  $m_K < 5.0$  mag, within a very high confidence level, correspond to stars of luminosity class I (Garzón *et al.* 1997), and a significant proportion of the remainder are very late giants which must also be rapidly evolving. We make the case, using all the available evidence, that we are observing a region at the nearer end of the Galactic bar, where the Scutum spiral arm breaks away, and that this is powerful evidence for the presence of the bar. Regions of this type can form due to the concentrations of shocked gas where a galactic bar meets a spiral arm, as is observed at the ends of the bars of many face-on external galaxies. Alternative explanations do not give nearly such a satisfactory account of the observations.

Equivalent spectroscopical analysis should also be performed at  $\ell = -22^\circ$ , the candidate position for the other tip of the bar. The space localization of one and, *a fortiori*, of both ends of the bar allows us to infer its orientation. If the second region is also confirmed to be a powerful star formation region this would imply a position angle for the bar of  $\sim 75^\circ$  with respect to the Sun–Galactic centre line. This geometry is indeed compatible with the range of distances

that we have obtained for the star-forming region at  $\ell = 27^\circ$  from spectroscopic parallaxes. However, the angle is different from that given by other authors for the bar and this, we think, is because they refer to the triaxial bulge and not to the bar as detected here.

*Subject headings:* stars: formation – Galaxy: stellar contents – Galaxy: structure

## 1. Introduction

This paper is the second part of Garzón *et al.* (1997) (hereafter G97) in which we presented an outline of the analysis of 60 spectra from a follow-up program to the TMGS project in the  $\ell = 27^\circ$ ,  $b = 0^\circ$  area. This analysis was based on the luminosity classification of stars using the CaII triplet (Jones *et al.* 1984; Díaz *et al.* 1989), and a discussion of this region was presented which strengthens the identification of this zone as a star formation region at the receding tip of the stellar bar.

In this second paper, we present the spectra, offer a more detailed explanation of the analysis, and supply a more complete information for each of the 60 stars, extended bibliography, and further discussions of the physical morphology.

## 2. Observations and data reduction

As explained in G97, 70 spectra of stars situated in the region around  $\ell = 27^\circ$ ,  $b = 0^\circ$  selected from the TMGS with  $m_K < 5.0$  mag were taken with the Isaac Newton Telescope in La Palma (Canary Islands, Spain). From these, we had to reject ten which could not be identified as visible counterparts of TMGS sources. After cross-correlating the original TMGS source positions with their *Guide Star Catalogue* counterparts and then calculating the errors in position, we inferred that TMGS catalog has a positional error box of around 4 arcsec in right ascension by 7 arcsec in declination. The larger error in declination compared with that in right ascension is due to the form of detector array used in the survey (Garzón *et al.* 1993). This is added to the pointing error of the INT telescope itself and implies that there is a non-negligible risk of taking the spectrum of the wrong star in such a very crowded area of the sky. By taking spectra of all the bright stars within the error box, we could decide *post hoc* which candidate was the TMGS object with  $m_K < 5.0$  mag from the

spectral type and features and  $I$ -magnitude estimate. In the ten cases mentioned above, we could not find any good candidate so these were rejected.

In Table 6 and Fig. 2, coordinates of all the stars in our sample from the TMGS database are given. Investigators who may wish to use them should be aware that, due to the error of the TMGS coordinates described above, and the extremely crowded nature of the field there is often more than one visible candidate for the infrared source. As we did not use more precise coordinates for a given source, we have not needed to sharpen the precision of these positions.

The extraction of the spectra, the sky subtraction and the wavelength calibration were performed using the IRAF tasks `apextract` and `onedspec` after performing the bias subtraction and the flat fielding with `ccdred`. The flux was normalized rather than calibrated.

### 3. Luminosity classification

Spectra in the zone of the IR Ca II triplet at 8498.02 Å, 8542.09 Å, and 8662.14 Å, present in stars of spectral types later than F5, were examined. The triplet was chosen as an optimum differentiator between stars of different luminosity classes. In earlier types, the Paschen hydrogen lines P13 (8665 Å), P15 (8545 Å) and P16 (8502 Å) severely contaminate the spectral region of interest. For spectral types later than M3 or M4, TiO absorption bands mask the Ca II triplet, making its features more difficult to measure, as we will see later.

Measurement of the equivalent width of the Ca II triplet lines was carried out according to the prescriptions of Díaz *et al.* (1989) when TiO-band contamination is not present. A continuum  $I_{\lambda}^{\text{cont}}$  is defined by a linear fit to the median value of two chosen side-bands

centered at 8455 Å and 8850 Å, respectively, with a width of 15 Å and the equivalent width was obtained by integrating:

$$W_{\lambda} = \int_{\lambda-15\text{Å}}^{\lambda+15\text{Å}} \left( 1 - \frac{I_{\lambda'}}{I_{\lambda'}^{\text{cont}}} \right) d\lambda', \quad (1)$$

where  $I_{\lambda}$  is the measured intensity.

We also followed Díaz *et al.* (1989) in defining

$$\text{EW} = W_{8542 \text{ Å}} + W_{8667 \text{ Å}} \quad (2)$$

as the indicator of luminosity class. The shortest-wavelength line of the triplet was not used because it is too feeble compared with the neighboring features and yields larger errors in the precise measurement of the total CaII triplet. Selected reference stars were used to check our EWs and these were the same, within the error margin, as those given by Díaz *et al.* (1989) for the same objects.

The CaII triplet has been used for many years as an indicator of luminosity class (*e.g.*, Merrill 1934). More recently Jones *et al.* (1984), and Díaz *et al.* (1989) have calibrated empirically the relationship between the equivalent width of the Ca II triplet and the luminosity class for spectral types ranging from F5 to M3. These authors found some dependence of EW on both metallicity and temperature, but these effects were much weaker than the dependence on surface gravity, especially for supergiants. We have followed their results and adopted their criteria in assigning luminosity classes from the measured EWs. From Díaz *et al.* (1989), if metallicity dependence is assumed negligible, then

$$\log g = 7.75 - 0.65\text{EW}. \quad (3)$$

On this basis, a source is taken to be a supergiant ( $\log g$  less than approximately 1.75) if  $\text{EW} > 9 \text{ Å}$ , independently of metallicity and temperature. Idiart *et al.* (1997) have

demonstrated the presence of correlations of EW with metallicity and temperature, but only for old stars ( $> 1$  Gyr), and therefore not for supergiants. There are also other possible luminosity-class indicators. In the wavelength range we used, the existence of the CN band (7916–7941 Å) is a characteristic of supergiants (MacConnell *et al.* 1992), but the Ca II triplet is less affected by noise.

Thirty-eight stars in the sample were not contaminated by the TiO band, and we used the method described above to obtain their EWs in this subsample (see Table 6).

The remaining 22 stars are of later spectral types, and the presence of TiO bands partially masks the triplet lines (see Fig. 6 *c*), *d*). For these objects we have developed an empirical method which permits the measurement of EW where the Ca II lines are not completely masked by the TiO band. This method uses the depth of the lines instead of the EW.

The depth of the lines is calculated according to

$$\text{depth}_\lambda = 1 - \frac{\min(I_{\lambda'}; \lambda - 15 \text{ Å} < \lambda' < \lambda + 15 \text{ Å})}{I_\lambda^{\text{cont2}}}, \quad (4)$$

where  $I_\lambda^{\text{cont2}}$  is the value of a new continuum interpolated between two points that are not affected by the TiO absorption: 8432 Å and 8844 Å <sup>1</sup>.

One potential problem is that the convolution of the profiles of the spectral lines with the instrumental profile would affect the depth of the line but this effect is in practice negligible compared with the other uncertainties in the method. The convolution with the instrumental profile broadens the line and decreases the depth when the number of pixels

---

<sup>1</sup>In fact, a bandwidth of 15 Å between 8417 Å and 8432 Å is selected for which we calculate the median value, and the same is done for the second value of the continuum between 8844 Å and 8859 Å.

defining the line is small. In the lines without TiO contamination, the pixels defining a line cover a sufficient wavelength range for the effect of the convolution to be negligible. In the lines with TiO contamination, the depth is the sum of the TiO band depth and the jump between the TiO band and the peak of the line. If the unblended portion of the line covers a restricted wavelength range, this jump will be affected by the convolution but, as it is small compared with the TiO depth, the effect of the convolution is again small. The effect of convolution would indeed be serious if we were to use Gaussian fits on masked portions of the lines instead of the depth as the measure of equivalent width.

To get the EW as a function of the depth of the deepest line, 8542 Å, it is necessary to use uncontaminated lines. Expression (4) is used for the first 38 stars, those with unmasked CaII lines, and for these a relationship is then calibrated between  $\text{depth}_{8542}$  and the EW calculated using eq. (2). The relationship obtained, employing a linear fit, was:

$$\text{EW} = -0.1 + 17.8 \times \text{depth}_{8542}, \quad (5)$$

which is plotted, together with the data, in Figure 2<sup>2</sup>. The use of this expression to evaluate the luminosity class using the criterion of Díaz *et al.* (1989) is a fair approximation. The fit in equation (5) is a good approximation but in the latest spectral types other effects may intervene. The equivalent width of the Ca II triplet is not strongly dependent on spectral type, although this dependence is a little more noticeable for M-type stars since

---

<sup>2</sup>The fit to a second-degree polynomial was  $\text{EW} = -7.1 + 45.0 \times \text{depth}_{8542} - 25.8 \times \text{depth}_{8542}^2$  which is very close to the linear fit and yields the same values, within the error limits. We emphasize that in G97 we used a second-degree fit, but with a small error, which gave rise to EW values too low by 0.2 or 0.3 Å. This led to our classifying two stars as giants instead of supergiants. This improved result only strengthens our previous conclusions about the proportion of supergiants in the sample.

the ionization equilibrium in these objects shifts somewhat from Ca II to Ca I (Cohen 1978). One consequence is that this line-depth technique may slightly underestimate the number of supergiants. That is, the number of supergiants among stars later than M3 may well be in fact larger than that inferred using the  $EW > 9$  criterion applied to equation (5). Since our purpose is to calculate the fraction of supergiants to determine whether the region studied is a star-formation region, this underestimate could change our conclusion only if the answer were negative, but this is not the case, as will be shown below.

Even employing the line-depth technique, we had to reject two stars of the sample for which the TiO band gave an unacceptable blend, so we finished with 58 stars—38 earlier than M3, and 20 later than M3—with acceptable EWs. The two stars rejected show spectra with no clearly unblended CaII features; the Ca II+TiO blends show a maximum depth<sub>8542 Å</sub> from which we may estimate a maximum EW. In both cases, this maximum value of EW is  $\approx 10.2$  Å, i.e.  $EW < 10.2$ , so it could not be decided whether they are giants ( $EW < 9.0$ ) or supergiants ( $EW > 9.0$ ). In Table 6, we do show the data for these two stars with  $EW < 10.2$  (stars 29 and 37) but these are not included in either the statistics of the EW or in the distance calculation of paper G97.

The final results of the luminosity classification were shown in Fig. 1 of G97, in the form of a histogram of EW frequencies. Those EW values used for the figure are shown in Table 6 for each star.

The ratio of SGs—those with  $EW > 9$  Å—to the total number of observed objects is most striking. The number of SGs is in fact 38 out of 58 (66%). In a binomial distribution the root mean square of the distribution is  $\sigma = \sqrt{n \times p \times (1 - p)}$ , where  $n$  is the total number of stars. Here,  $n = 58$  stars,  $p = 0.66$ , so  $\sigma = 3.6$  stars. The proportion of supergiants is then  $66 \pm 6\%$  ( $1 \sigma$ ). An error should be added to allow for the possible mistaken classification of giants and supergiants, and also to take into account the pointing

error of the telescope in a crowded field which gives a slight chance of taking the spectrum of a wrong star. However, if the “wrong” star turned out to be a late star with sufficient luminosity to give a spectrum of bright star, this would still be indication of late type giants and supergiants in the zone. These sources of error are small except in the M-type classification, in which the number of supergiants should be even greater than given by our criterion, as discussed before. These considerations lead to the conclusion that the fraction of supergiants is well over 50% with a very high confidence level.

#### 4. Spectral classification

The spectra of the 60 stars belonging to both subsamples are presented in Fig. 6, after removing the intrinsic slopes and those due to reddening, in order to show the qualitative differences in the spectra between different kinds of stars. The spectral type classification is carried out for every star by qualitatively comparing the features of our spectra with those of standard stars. The spectral classification is shown in Table 6.

The coolest stars—M3 and later on—were compared with those in Bessel (1991), Schulte-Ladbeck (1988), and Barbieri *et al.* (1981), by inspecting the depth of the TiO band absorption. In Fig 6 *c*) and *d*), it can be seen that there is a growing depression at 8432 Å and 8844 Å from M3 to M9. Since the features of these sources permit us to differentiate spectral types with an interval of 0.1 or 0.2 spectral types, the classification is quite accurate for these stars.

The earlier-type stars were compared with those in Torres-Dodgen & Weaver (1993), and Schulte-Ladbeck (1988), mainly by inspecting lines such as Mg I 8807 Å, Fe I 8612 Å, Fe I–Ti I 8468 Å, O I–Fe I 8446 Å (some of these features are also dependent on luminosity class or metallicity) and Paschen hydrogen lines for those earlier than G2. In this case the

errors in the classification could be as large as half a spectral type, except perhaps for those containing Paschen lines.

A histogram of the frequency of spectral types in our sample is shown in Figs. 2 and 3 of G97. As expected, most of the stars are very red and with intrinsic luminosity (see also Calbet *et al.* 1996a) since TMGS is more sensitive to redder stars. The predominant type among the supergiants is K. Supergiants of very late types are known to exist in very small numbers; we have found a significant number of new examples here. This result is subject to the bias that our method of predicting the EWs gives where the TiO band affects the Ca II lines; it tends to underestimate the EWs, thereby reducing the apparent fraction of SGs in the coolest (M) class.

## 5. Stellar bar

The conclusion arised from this analysis is that the observed region contains intense star formation of recent origin, since supergiants and bright giants are necesarily young stars. There is a high proportion of young stars, and their high spatial concentration shows that the star formation has taken place in the zone observed. Any associated early B-type or O-type stars, typical of this kind of cluster, are not observed in this case since their emission in  $K$  is too low to reach  $m_K < 5$  mag for objects far from the solar neighborhood, and the emission in the visible is very strongly affected by dust extinction.

This star formation region does not belong to the disc nor the spiral arms (G97); nor it is likely belonging to the ring, as exposed in G97 and Hammersley *et al.* (1994) (hereafter H94). A further convincing reason for excluding a ring, even an elliptical one, besides the ones in those papers, is that it would be prominent in other TMGS regions closer to the center than  $\ell=27^\circ$ , and that the luminosity function of the stellar excess

would be invariant, neither of which would be in agreement with the observations. The TMGS star counts after subtraction of a model disc (Wainscoat *et al.* 1992) and bulge (López-Corredoira *et al.* 1997) are zero in off-plane directions, showing that those disk and bulge models are good fits to the observations; there is, however, an excess of stars in the plane ( $|b| < 2^\circ$ ). Figure 5 shows a sharp decrease in the star counts in the center, and also that the luminosity function of the stellar excess at  $\ell=27^\circ$  is different from that in the other regions (the ratio between stars with  $m_K \leq 9.0$  mag and  $m_K \leq 5.0$  mag is very different). These considerations lead to the conclusion that a ring-type structure, even elongated and eccentric, gives a poor fit to the observations.

A hole in the extinction was suggested as a possible cause of the excess at  $\ell=27^\circ$  by Jones *et al.* (1981) but this idea was criticized by Kawara *et al.* (1982) who observed an invariant (H-K) colour for the stars across this region. Also, the TMGS star counts at  $\ell=27^\circ$  in the plane show an excess of over 100 stars per square degree up to  $m_K = 5$  and this cannot be satisfactorily explained by assuming that the extinction is zero in that region, according to our calculations. Furthermore, CCD *VRI* photometry of the region shows clearly that the line-of-sight extinction is greater than the standard value of 0.62 mag  $\text{kpc}^{-1}$  in V (Mahoney 1999, Hammersley *et al.* 1998).

The most likely explanation is the presence of a giant star formation region which is associated with the receding tip of the stellar Galactic bar (see Fig. 3). If we take the region to be in the center of the star formation region at the end of a bar<sup>3</sup>, it can be used not only as a qualitative demonstration of the bar’s existence but also as a means to

---

<sup>3</sup>Its center is at  $\ell \sim 27^\circ$ ,  $b \sim 0^\circ$ . More precisely, Viallefond *et al.* (1980) places the region with center at  $\ell = 27.5^\circ$ . The region is extended over several degrees but this is the point where the star counts show a maximum which we believe correspond to the center.

estimate its orientation. The remaining stars in Fig. 5 can be explained as bar stars, with a prominent peak at both ends due to the interaction with spiral arms. Such regions can form due to the concentrations of shocked gas where the Galactic stellar bar meets a spiral arm, as is observed at the ends of the bars of face-on external galaxies (Sandage & Bedke 1994). An excess of extinction at negative latitudes (Calbet *et al.* 1996b) is also explained by the stellar-bar hypothesis.

This is not the first time that a Galactic bar has been claimed to be discovered but our arguments in favour of it are new and different from those of other authors. De Vaucouleurs (1964, 1970) first suggested that the Galaxy might be barred in an attempt to explain the observed non-circular gas orbits. Since then, many types of observational evidence have been accumulated that support this hypothesis (see Blitz 1993; Blitz *et al.* 1993; Kuijken 1996a; Gerhard *et al.* 1997). The axial asymmetry of the inner Galaxy is detected by star counts (Nakada *et al.* 1991; Weinberg 1992; Whitelock *et al.* 1992; Stanek *et al.* 1994, 1996; Wózniać & Stanek 1996; Nikolaev & Weinberg 1997), or by surface photometry at different wavelengths (Blitz & Spergel 1991; Weiland *et al.* 1994; Dwek *et al.* 1995, Sevenster 1996), stellar population studies in Baade’s window (Ng *et al.* 1996), micro-lensing (Paczynski *et al.* 1994) and studies of the extinction using lensed stars (Stanek 1995), analysis of internal motions of the gas (Peters 1975; Liszt & Burton 1980; Yuan 1984; Gerhard 1996). Models including a bar (*e.g.*, Binney *et al.* 1991; Zhao 1996) can explain these observational features.

Not all of these observations necessarily imply the existence of a bar; some could be explained by a triaxial structure in the inner Galaxy. Whether this structure is a triaxial bulge, or whether a bar or both features are present is still a matter of controversy (Kuijken 1996b; Ng 1997), and there are reasons for believing that many authors who refer to a bar are in fact referring to the triaxial bulge.

In our previous analysis of the Two Micron Galactic Survey (TMGS) database (Garzón *et al.* 1993) we described evidence in favor of the presence of a triaxial bulge (López-Corredoira *et al.* 1997) with radial scale length  $\sim 2.2$  kpc, making an angle  $12^\circ$  with respect to the Sun–Galactic center line in the first quadrant, in strong agreement with the angle given by many of other authors (Binney *et al.* 1991; Weinberg 1992; Dwek *et al.* 1995; Binney *et al.* 1997; Stanek *et al.* 1997; Nikolaev & Weinberg 1997) whose bar angle (around 20 degrees) is quite close to this. The bar of this paper must be a different structure from the triaxial bulge since the inclination of the bulge is not sufficient for a bar tip to reach  $\ell = 27^\circ$  nor for a dust lane to reach  $\ell = -19^\circ$  at the other side of the bar, as found by Calbet *et al.* (1996b). The triaxial bulge reported by López-Corredoira *et al.* (1997) does not yield sufficient star counts in the plane at positive Galactic latitudes, taking into account the disk and the extinction, to explain the observations.

There is another infrared peak at negative Galactic longitudes: at  $\ell = -22^\circ$ , which is very similar to the one analyzed here<sup>4</sup>. If we assume that the other end of the bar is at  $\ell = -22^\circ$ , the orientation of the bar can be derived. In fact, it is a simple trigonometrical problem when we take the bar to be rectilinear and with equal length from each end to the center.

Applying the sine rule (see Fig. 4),

$$\frac{L_0}{\sin 27^\circ} = \frac{R_0}{\sin(180^\circ - 27^\circ - \alpha)}, \quad (6)$$

---

<sup>4</sup>See *COBE*-DIRBE data (Boggess *et al.* 1992) or near-infrared catalogs which cover the Galactic plane at positive and negative Galactic longitudes. See also H94, and Calbet *et al.* (1996b).

$$\frac{L_0}{\sin 22^\circ} = \frac{R_0}{\sin(\alpha - 22^\circ)}. \quad (7)$$

Hence, with  $R_0 = 7.86$  kpc (López-Corredoira *et al.* 1997), we deduce that  $\alpha = 75.6^\circ$  and the length of the bar from tip to tip is  $2L_0 = 7.4$  kpc.

Therefore, we suspect that the authors which are giving a much lower angle are in fact analysing the angle of the triaxial bulge, or an average angle of the composition of both bulge and bar, instead the bar angle. The triaxial bulge cannot be causing the features seen at  $\ell = 27^\circ$ .

We can also derive geometrically the distance to the tip at  $\ell = 27^\circ$  as being 7.8 kpc. This distance is compatible with that derived in G97 (in table 6 are the distances for each star), taking into account all the uncertainties in the calculation.

## 6. Conclusions

This paper, together with its first part (G97) makes a spectroscopic analysis of the brightest stars in an infrared selected sample of objects close to the Galactic plane at  $\ell = 27^\circ$  showing a strikingly high fraction of supergiants, characteristic of a strong star formation region.

We argue, using all the available evidence, that this region is situated at one end of the Galactic bar, where the Scutum spiral arm breaks away, and that the presence of the region is itself a powerful evidence for the presence of the bar. None of the alternative possibilities (arm, disk, bulge or ring components) is capable of explaining the observations in a satisfactory manner.

The detected presence of a similar concentration of near-IR sources in the plane at

$\ell = -22^\circ$  should, on this hypothesis, indicate the other end of the bar. To confirm this requires a similar spectroscopic campaign to that reported here. A rectilinear bar between these two points makes an angle of  $75^\circ$  with the Sun–Galactic centre line, and has a total length of 7.4 kpc. The distance this implies to the star-forming zone analyzed here is consistent with the estimated spectroscopic parallaxes of the stars whose spectra we have analyzed in the first part of the paper (G97), giving a self-consistent picture of the bar.

It is important to distinguish this bar from the triaxial bulge of the Galaxy (López-Corredoira *et al.* 1997). Many of the previous claims to describe a Galactic bar are more likely to refer to the triaxial bulge and not to the bar.

The Isaac Newton Telescope is operated on the island of La Palma by the Royal Greenwich Observatory in the Spanish Observatorio del Roque de Los Muchachos of the Instituto de Astrofísica de Canarias. This work was partially supported by grants PB94-1107, and PB97-0219 of the Spanish DGICYT.

## REFERENCES

- Barbieri C., Bonoli C., Bortoletto, F., di Serego, S., Falomo, R. 1981, *Mem. Soc. Astron. Italiana*, 52, 195
- Bessel, M. S. 1991, *AJ*, 101, 662
- Binney, J., Gerhard, O. E., Stark, A. A., Bally, J., Uchida K. I. 1991, *MNRAS*, 252, 210
- Binney, J., Gerhard, O. E., Spergel, D. 1997, *MNRAS*, 288, 365
- Blitz, L. 1993, in *AIP Conf. Proc.* 278, *Back to the Galaxy*, ed. S. S. Holt and F. Verter (New York: AIP), p. 98
- Blitz, L., Binney, J., Lo, K. Y., Bally, J., Ho P. T. P. 1993, *Nat*, 361, 417
- Blitz, L., Spergel, D. N. 1991, *ApJ*, 370, 205
- Bogges, N. W. et al. 1992, *ApJ*, 397, 420
- Calbet, X., López-Corredoira M., Hammersley P. L., et al., 1996a, in: *New Extragalactic Perspectives in the New South Africa*, D. L. Block, J. Mayo Greenberg, eds., Kluwer, Dordrecht, p. 532
- Calbet X., Mahoney T., Hammersley P. L., Garzón F., López-Corredoira, M. 1996b, *ApJ* 457, L27
- Cohen J. G., 1978, *ApJ* 221, 788
- Cohen M., 1994, *Ap&SS* 217(1), 181
- de Vaucouleurs G., 1964, in: *The Galaxy and the Magallanic Clouds*, IAU Symp. 20, eds. F. J. Kerr & A. W. Rodgers (Sydney, Aust. Acad. Sci.), p. 195

- de Vaucouleurs G., 1970, in: The Spiral Structure of Our Galaxy, IAU Symp. 38, W. Becker, G. Contopoulos, eds., Reidel, Dordrecht, p. 18
- Díaz A. I., Terlevich E., Terlevich R. 1989, MNRAS 239, 325
- Dwek E., Arendt R. G., Hauser M. G., et al., 1995, ApJ 445, 716
- Garzón F., Hammersley P. L., Mahoney T., et al., 1993, MNRAS 264, 773
- Garzón F., López-Corredoira M., Hammersley P. L., et al., 1997, ApJ 491, L31 (G97)
- Gerhard O. E., 1996, in: Unsolved Problems of the Milky Way, IAU Symp. 169, eds. L. Blitz, P. Teuben, Kluwer, Dordrecht, p. 79
- Gerhard O. E., Binney J., Zhao H., 1997, preprint astro-ph/9710361
- Hammersley P. L., Garzón F., Mahoney T., Calbet X., 1994, MNRAS 269, 753 (H94)
- Hammersley P. L., Garzón F., Mahoney T., López-Corredoira M., 1998, in: The Impact of Near-infrared Sky Surveys on Galactic and Extragalactic Astronomy, ed. N. Epchtein, Kluwer, Dordrecht, p. 63
- Idiart T. P., Thévenin F., Freitas Pacheco J. A. de, 1997, AJ 113(3), 1066
- Jones J. E., Alloin D. M., Jones B. J. T., 1984, ApJ 283, 457
- Jones T. J., Ashley M., Hyland A. R., Ruelas-Mayorga A., 1981, MNRAS 197, 413
- Kawara K., Kozasa T., Sato S., et al., 1982, PASJ 34, 389
- Kuijken K., 1996a, in: Barred galaxies, IAU symp. 157, Buta R., Crocker D. A., Elmegreen B. G., eds., ASP conference series, San Francisco, p. 504
- Kuijken K., 1996b, in: Unsolved problems of the Milky Way, IAU Symp. 169, L. Blitz, P. Teuben, eds., Kluwer, Dordrecht, p. 71

- Liszt H. S., Burton W. B., 1980, ApJ 236, 779
- López-Corredoira M., Garzón F., Hammersley P. L., Mahoney T. J., Calbet X., 1997, MNRAS 292, L15
- MacConnell D. J., Wing R. F., Costa E., 1992, AJ 104(2), 821
- Mahoney T. J., 1999, in preparation
- Merrill P. W., 1934, ApJ 79, 183
- Nakada Y., Deguchi S., Hashimoto O., et al., 1991, Nat 353, 140
- Ng Y. K., 1997, preprint astro-ph/9709196
- Ng Y. K., Bertelli G., Chiosi C., Bressan A., 1996, A&A 310, 771
- Nikolaev S., Weinberg M. D., 1997, ApJ 487, 885
- Paczynski B., Stanek K. Z., Udalski A., et al., 1994, ApJ 435, L113
- Peters W. L., 1975, ApJ 195, 617
- Sandage A., Bedke J., 1994, The Carnegie Atlas of Galaxies, Carnegie Institution of Washington, Washington
- Schulte-Ladbeck R. E., 1988, A&A 189, 97
- Sevenster M. N., 1996, in: Barred galaxies, IAU symp. 157, Buta R., Crocker D. A., Elmegreen B. G., eds., ASP conference series, San Francisco., p. 536
- Space Telescope Science Institute, 1992, The Guide Star Catalog version 1.1, Baltimore.
- Stanek K. Z., 1995, ApJ 441, L29
- Stanek K. Z., Mateo M., Udalski A., et al., 1994, ApJ 429, L73

- Stanek K. Z., Mateo M., Udalski A., et al., 1996, in: Barred galaxies, IAU symp. 157, Buta R., Crocker D. A., Elmegreen B. G., eds., ASP conference series, San Francisco, p. 545
- Stanek K. Z., Udalski A., Szymański M., et al., 1997, ApJ 477, 163
- Torres-Dodgen A. V., Weaver W. M. B., 1993, PASP 105, 693
- Viallefond F., Wijnbergen J. J., Lena P., et al., 1980, A&A 83, 22
- Wainscoat R. J., Cohen M., Volk K., Walker H. J., Schwartz D. E.; 1992, ApJS 83, 111
- Weiland J. L., Arendt R. G., Berriman G. B., et al., 1994, ApJ 425(2), L81
- Weinberg M. D., 1992, ApJ 384, 81
- Whitelock P. A., Feast M. W., Catchpole R. M., 1991, MNRAS 248, 276
- Woźniak P. R., Stanek K. Z., 1996, ApJ 464, 233
- Yuan C., 1984, ApJ 281, 600
- Zhao H., 1996, in: Barred galaxies, IAU symp. 157, Buta R., Crocker D. A., Elmegreen B. G., eds., ASP conference series, San Francisco., p. 549

## FIGURE CAPTIONS

**Figure 1:** Equatorial coordinates (J2000) of the stars whose spectra are analyzed in this paper. Small circles stand for giants and big circles stand for supergiants.

**Figure 2:** Comparison between  $EW$  measured in unmasked CaII lines using (2) and the subsample having the  $EW$  obtained via (5).

**Figure 3:** TMGS star counts as functions of Galactic longitudes in the Galactic plane after subtraction of the Wainscoat et al. (1992) model disc and the López-Corredoira et al. (1997) model bulge.

**Figure 4:** A bar can explain a number of observations: the excess of extinction at negative Galactic latitudes due to a dust lane (Calbet et al. 1996b), and the star formation regions at each end of the bar.

**Figure 5:** Geometry of the bar sustaining an angle  $\alpha$  with respect to the Sun (S)-Galactic center (C) line.

**Figure 6:** Plots of the spectra from our sample in the range 7900Å- 8900Å. The intrinsic slopes and those due to reddening have been removed. Numbers for the stars in the right hand side correspond to those given in the first column of the Table 6, and the spectral type and luminosity class of the star.

—